Effect of Magnetite Nanoparticles Content on the Magnetic Properties of Polylactide and Polystyrene Composites

Armando Galluzzi[a,b], Marius Murariu[c], Jean-Marie Raquez[c], Philippe Dubois,[c] Massimiliano Polichetti[a,b]

[a]Department of Physics "E.R. Caianiello", University of Salerno, via Giovanni Paolo II, 132, Fisciano (SA), I-84084, Italy
[b]CNR-SPIN Salerno, via Giovanni Paolo II, 132, Fisciano (SALERNO), I-84084, Italy
[c]University of Mons & Materia Nova R&D Centre, Mons - 7000, Belgium
agalluzzi@unisa.it

The effect of magnetite nanoparticles (NPs) content on the magnetic properties of polylactide (PLA) and polystyrene (PS) matrix has been investigated by means of DC magnetization measurements as a function of temperature (T) and magnetic field (H). Previous to the dispersion by melt-compounding into PLA and PS, the magnetite NPs have been reactively surface treated with 3% polymethylhydrogensiloxane (MHX) in order to make them hydrophobic and more stable to the action of oxygen and moisture. The magnetic analysis of the properties has been performed by measuring the Zero Field Cooling (ZFC) magnetization curve as a function of the temperature, at 0.1 Tesla applied field. In this framework, a superparamagnetic shape like has been noted for all the samples with the possibility to individuate the blocking temperature (TB) of the NPs. Moreover, the magnetization as a function of the field has been measured at room temperature (in particular above TB) investigating the coercive field and the magnetization values finding potentially interesting results. In particular, the very low values obtained for the coercive field at room temperature, together with the maximum found in the ZFC curve, have confirmed the superparamagnetic behavior of the PLA and PS - magnetite filled samples. Finally, a table with the fundamental magnetic features values of the samples has been reported for understanding if the obtained results for this kind of surface treated NPs and the afferent nanocomposites could be suitable for being used in applications requiring superparamagnetic properties (protection of environment, magnetic microcarriers, magnetic separation of stem cells, other biomedical purposes).

1. Introduction

The interest of the scientific community in considering the magnetic NPs for various applications arise from the 1960s after the Bean and Livingstone dissertation about the superparamagnetic properties that the magnetic NPs can develop in certain conditions [Bean and Livingston, 1959]. In particular, in the last years, the possibility to embed the magnetic NPs in polymeric matrices produced considerable efforts in view of using these nanocomposites in many practical sectors ranging from environmental to biomedical ones [Shirinova et al., 2016; Zhu et al., 2013; Horst et al., 2016; Kalia et al., 2014]. The main magnetic features which make these samples so interesting are the high magnetic response in terms of magnetization and the coercive field close to zero that allows to use the magnetic NPs as drug delivery in cancer treatments even using small fields [Veiseh et al., 2010; Kim et al., 2010] or also in induced processes of hyperthermia of cancer cells [Hergt et al., 2006; Kumar and Mohammad, 2011]. Among all the magnetic NPs, the Fe_3O_4 (magnetite) ones are very attractive due to their biocompatibility and due to the fact that they show a low toxicity suggesting their possible use in data and energy storage sector [Zhang et al., 2010], in the enhancement of the contrast in magnetic resonance imaging [Huang et al., 2010], in the magnetic separation of stem cells [Balmayor et al., 2011] , as effective nanomaterials for the removal of heavy metals from water [Carlos et al., 2013; Kalia et al., 2014], and so on. Unfortunately, the magnetite NPs are very sensitive to the action of oxygen, thus some NPs might undergo oxidation to ferric hydroxide ($Fe(OH)_3$) or to maghemite ($\gamma\text{-}Fe_2O_3$) phases in an aqueous medium [Bini et al., 2012; Demirer et al., 2015]. To limit this undesired effect and also the aggregation of

primary NPs of low dimension (10-30 nm), specific surface treatments and techniques of encapsulation are currently used to allow their utilization [Oh and Park, 2011; Ali et al., 2016]. Also the choice of the polymeric matrix in which the NPs are embedded can be important for the exploit of their magnetic properties. Nowadays, the challenge of the researchers is to find the best category of polymers that can show biocompatibility, feasibility for applications and, finally, a low environmental impact. In this direction, among the polymers studied in the last decade, the bio-sourced polylactide (PLA) matrix has shown interesting characteristics together with other eco-friendly polymeric matrices [Murariu and Dubois, 2016; Dos Santos et al., 2015; Zhu et al., 2013; Kalia et al., 2014] that could substitute in some applications the petrochemical matrices, like the polystyrene (PS), which can be dangerous for the environment once degraded and because it requires a very long time for degradation [Ho et al., 2018]. On the other hand, due its stability and unique properties, PS is one of the main polymers currently used for encapsulation of magnetic nanoparticles and in biomedical applications [Yan et al., 2014; Lerman et al., 2018]. To propose as alternative the utilization of eco-friendly materials (i.e., PLA, bio-sourced, biocompatible and biodegradable) for applications requiring superparamagnetic properties, the studies were mainly focused on the production and characterization of PLA-magnetite nanocomposites, while the traditional PS (of petrochemical origin, non-biodegradable) and PS-based nanocomposites were used for comparative analyses.

In this work, the effect of Fe_3O_4 NPs content on the magnetic properties of PLA and PS nanocomposites have been analyzed by means of DC magnetic measurements as a function of the temperature and DC field, and the results have been discussed for understanding eventual suitability of the samples for applications.

2. Materials and methods

Poly(L,L-lactide)- produced by NatureWorks LLC (4032D grade), a general purpose PS (PS 158N, INEOS) and magnetite NPs with primary particle size in the range 20-30 nm (supplier IOLITEC) have been used as main raw materials. The nanofiller was reactively surface treated with 3% polymethylhydrogensiloxane (XIAMETER MHX-1107, Dow Corning) using a Rondol turbomixer, step followed by a specific curing treatment at 120°C (4h, under vacuum). For nanocomposites preparation, PLA was dry-mixed with up to 16% magnetite nanofiller, while the melt-compounding of blends was performed at 190°C (mixing 10 min, 150 rpm) using a twin-screw micro-compounder (Thermo-Scientific Haake MiniLab). The blends of PS and magnetite nanofiller were processed by melt-compounding at a temperature of 240°C, while in the subsequent step the PS nanocomposites have been used for comparative analyses. The two categories of samples have been characterized in DC magnetic field. The measurements have been performed by means of a Quantum Design PPMS equipped with a VSM option. The magnetization of the samples has been measured as a function of the temperature, M(T), and of the DC magnetic field, M(H). Before each measurement, the magnetic field has been reduced to 1×10^{-4} T as described elsewhere [Galluzzi et al., 2019, 2018b]. For what concerns the M(T) measurements, the sample has been cooled down to 5 K in absence of field and then the field has been put equal to H = 0.1 T. To perform the Zero Field Cooling (ZFC) curve, the temperature has been ramped from 5 K up to 300 K at 0.5 K/min [Iannone et al., 2007]. For what regarding the M(H) measurements, the temperature has been set to T = 300 K and stabilized for 30 minutes. After that, the magnetic field has been ramped from 0 T up to +9 T, from +9 T down to -9 T and finally from -9 T up to +9 T again to acquire the complete hysteresis loops [Galluzzi et al., 2018a].

3. Results and discussion

In order to study the influence of magnetite NPs content on the magnetic properties of nanocomposites, we have to understand firstly which is the magnetic behavior of the two pure samples of polylactide (PLA) and polystyrene (PS). At this aim, the hysteresis loops M(H) have been reported in Figure 1 for both the samples. A negative value of magnetization has been measured for both the materials when a positive magnetic field was applied. In particular, M(H = +9 T) = -0.035 emu/g for PLA and M(H = +9 T) = -0.068 emu/g for PS. This suggests a diamagnetic behavior of the neat samples. The magnetization measurements as a function of temperature M(T) have been performed on PLA samples filled with 4%, 8% and 16% of Fe_3O_4 NPs at a fixed field of 0.1 T and reported in Figure 2. Positive magnetization values can be seen together with the presence of a peak in the ZFC curves. These features in the M(T) curves suggest a superparamagnetic behavior of the samples. In the insets of Figure 2, the peak regions have been enlarged showing a blocking temperature (T_B) of about 150 K, 100 K, 150 K for the PLA samples filled with 4%, 8% and 16% of Fe_3O_4 NPs, respectively. The important aspect to consider in this kind of samples is the magnetic behavior for T > T_B since the NPs behaving in a superparamagnetic way can be exploited in a very wide range of applications ranging from technical to biomedical ones [Zhu et al., 2013; Di Palma et al., 2018; Horst et al., 2016; Polichetti et al., 2020;

Kalia et al., 2014]. For this reason, our field dependence magnetization analysis will be focused for $T > T_B$, in particular at room temperature (T = 300 K).
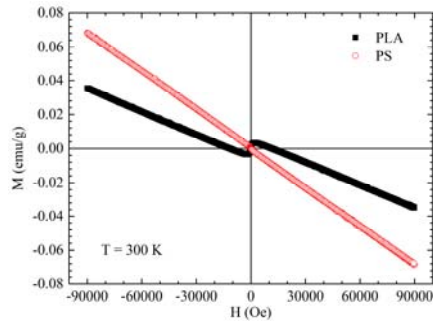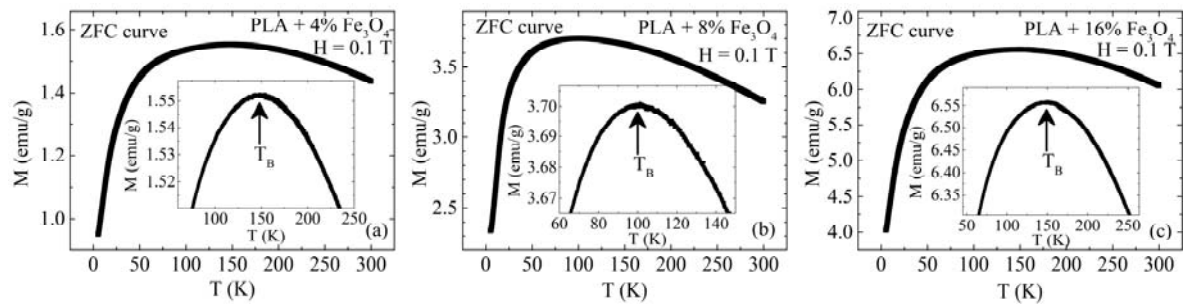

Figure 1: M(H) at T = 300 K on PLA and PS pure samples.

Figure 2: M(T) at H = 0.1 T on PLA + 4% Fe_3O_4 (a), PLA + 8% Fe_3O_4 (b), PLA + 16% Fe_3O_4 (c). Insets: the maximum in ZFC curve determines the blocking temperature T_B.

For what concerns the M(H) measurements, they have been performed for T = 300 K > T_B in order to study the superparamagnetic behavior of the samples. In particular, the M(H) curves for PLA + 4, 8, 16% Fe_3O_4 have been reported in Figure 3. Looking at high fields, it can be noted that the full saturation magnetization is not reached even at 9 Tesla although the 90% of the maximum signal is already reached at about 1.6-1.8 T for all the samples. These results suggest that there is the possibility to exploit almost completely the maximum magnetic response of the sample even at fields lower than its saturation field. A similar observation can be made considering that at H = 0.2 T, the 68% of maximum magnetization is reached. This is an important information since 0.2 T is a typically required field for biomedical applications [Pankhurst et al., 2003]. The inset of Figure 3 shows an enlargement of the near zero field region of the samples. It is important to note that the coercive field is low: $H_c = \pm 6$ Oe. This result is in agreement with the superparamagnetic behavior found in the M(T) curve and also suggests the good quality of the magnetite NPs in terms of small dimensions and superparamagnetic properties [Di Palma et al., 2018].
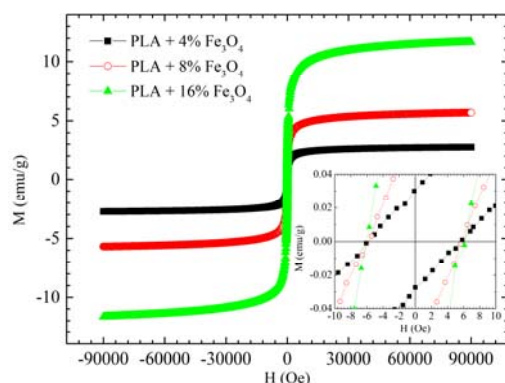

Figure 3: M(H) at T = 300 K on PLA + 4, 8, 16%Fe_3O_4. Inset: an enlargement of the region near zero field is shown.

Subsequently, we have reproduced the same measurement procedures for a representative PS filled sample for checking the differences and analogies among the PLA and PS samples. At this aim, in Figure 4 the M(T) for PS + 10% Fe_3O_4 has been reported. Also in this case, the sample presents positive magnetization values

that can be seen together with the presence of a peak in the ZFC curve. Again, these features in the M(T) curve suggest a superparamagnetic behavior of the sample. The blocking temperature for this sample is about 100 K (see inset Figure 4). It is worth to underline that the fact that the value of T_B being < 300 K allows to exploit the superparamagnetic properties of the sample at room temperature.
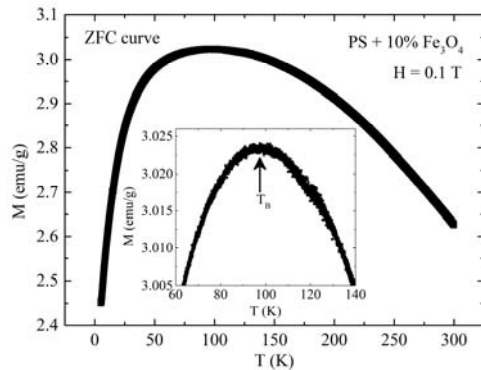

Figure 4: M(T) at H = 0.1 T on PS + 10%Fe₃O₄. Inset: the maximum in ZFC curve determines the blocking temperature T_B.

For what concerns the M(H) measurement, it has been performed for T = 300 K. The result is reported in Figure 5. The full saturation magnetization is not reached even at 9 Tesla although the 90% of the maximum signal is reached at 2 T. Another interesting feature is the magnetization percent at 0.2 T equal to 65% that can be exploited for biomedical applications (NB: value slightly lower than in the case of PLA – Fe₃O₄ nanocomposites). The inset of Figure 5 shows an enlargement of the region near zero field. It is important to observe that $H_c = \pm 5$ Oe, a very low value that indicates that the NPs have been well dispersed in the PS matrix so avoiding the agglomeration formation which would lead to high coercive fields and to the loss of the superparamagnetic properties.
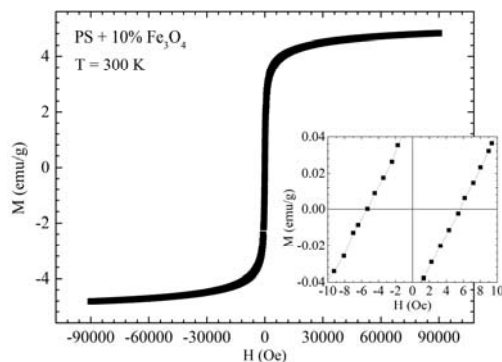

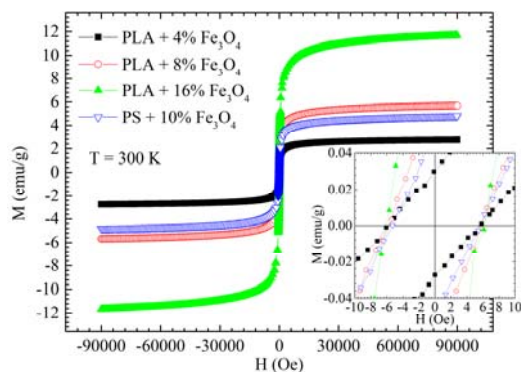Figure 5: M(H) at T = 300 K on PS + 10%Fe₃O₄. Inset: an enlargement of the region near zero field is shown.

Figure 6: M(H) at T = 300 K for all the considered samples. Inset: the region near zero field is shown.

A direct comparison of the M(H) curves among all the samples at T = 300 K is provided in Figure 6. In the main panel it is interesting to note that no samples reach the magnetic saturation, even at 9 T. Another feature to observe is that the PS + 10% Fe_3O_4 presents a magnetization always lower than PLA + 8% Fe_3O_4 despite having a higher Fe_3O_4 concentration, aspect that will require carefully explanation taking into account the influence of different factors (nature of polymer matrix, quality of distribution and dispersion of NPs, presence or not of specific additives, others). On the other hand, in the inset of Figure 5 the behavior of all the samples near zero field has been reported. It can be observed that all the values are similar and near to zero indicating a superparamagnetic behavior for all the samples.

The key magnetic parameters extracted from the measurements are summarized in Table 1. The magnetic features reported in Table 1 can be compared quite favorably with those of other formulations [Shannigrahi et al., 2012; Dos Santos et al., 2015; Wilson et al., 2004; Shirinova et al., 2016] although the complexity of a fair comparison due to differences in filler type, size, shape and content that affect the magnetic properties of the samples. The Table shows that, in principle, both the PLA and PS -magnetite nanocomposites have magnetic properties suitable for the various applications mentioned in the introductive section. Nevertheless, it is worth to underline that the PLA use is advisable from an environmental point of view due to its biocompatibility and biodegradability (NB: leading to carbon dioxide (CO_2), water and humus as final products of biodegradation) with respect to the PS that has a petrochemical origin and so hypothetically harmful to the environment as source of toxic chemicals once degraded.

Table 1: Magnetic features of the samples at T = 300 K.

Sample	Coercive field (Oe)	Percent of M_{max} @ H = 0.2 T	H (90% M_{max}) (T)	H (M_{sat}) (T)
PLA + 4% Fe_3O_4	± 6	68	1.6	> 9
PLA + 8% Fe_3O_4	± 6	68	1.7	> 9
PLA + 16% Fe_3O_4	± 6	68	1.8	> 9
PS + 10% Fe_3O_4	± 5	65	2	> 9

4. Conclusions

The DC magnetic properties of PLA and PS matrices filled with different percentages of Fe_3O_4 NPs have been studied as a function of temperature and magnetic field. For all the samples, a superparamagnetic behavior has been found analyzing the M(T) and M(H) curves. In particular, from the ZFC curves of M(T) measurements a blocking temperature well below 300 K has been found for all the samples indicating the possibility to exploit the superparamagnetic features of the samples at room temperature. In this framework, the magnetization of the samples has been studied as a function of magnetic field at T = 300 K finding very low coercive fields, about 5-6 Oe, in agreement with the superparamagnetic behavior observed in the M(T) curves. Moreover, it has been observed that the full saturation magnetization was not reached even at 9 Tesla although the 90% of the maximum signal can be achieved for H ≤ 2 T for all samples. Another important characteristic of all the samples consists in the fact that almost the 70% of the Magnetization can be exploited at H = 0.2 T suggesting the possibility to use these samples also in biomedical applications. Finally, a table with the fundamental magnetic features values has been reported showing that the PLA composite samples are characterized by outstanding magnetic properties, thus they are preferable for utilization in various applications for the protection of environment thanks to their biocompatibility and biodegradability.

References

Ali A, Zafar H, Zia M, ul Haq I, Phull AR, Ali JS, Hussain A. 2016. Synthesis, characterization, applications, and challenges of iron oxide nanoparticles. Nanotechnol. Sci. Appl. 9: 49–67.

Balmayor ER, Pashkuleva I, Frias AM, Azevedo HS, Reis RL. 2011. Synthesis and functionalization of superparamagnetic poly-ε- caprolactone microparticles for the selective isolation of subpopulations of human adipose-derived stem cells. J. R. Soc. Interface 8: 896–905.

Bean CP, Livingston JD. 1959. Superparamagnetism. J. Appl. Phys. 30: S120–S129.

Bini RA, Marques RFC, Santos FJ, Chaker JA, Jafelicci M. 2012. Synthesis and functionalization of magnetite nanoparticles with different amino-functional alkoxysilanes. J. Magn. Magn. Mater. 324: 534–539.

Carlos L, Garcia Einschlag FS, C. M, O. D. 2013. Applications of Magnetite Nanoparticles for Heavy Metal Removal from Wastewater. In: Waste Water - Treatment Technologies and Recent Analytical Developments. InTech.

Demirer GS, Okur AC, Kizilel S. 2015. Synthesis and design of biologically inspired biocompatible iron oxide nanoparticles for biomedical applications. J. Mater. Chem. B 3: 7831–7849.

Galluzzi A, Buchkov K, Tomov V, Nazarova E, Leo A, Grimaldi G, Nigro A, Pace S, Polichetti M. 2018a. Evidence of pinning crossover and the role of twin boundaries in the peak effect in FeSeTe iron based superconductor. Supercond. Sci. Technol. 31: 015014.

Galluzzi A, Buchkov KM, Nazarova E, Tomov V, Grimaldi G, Leo A, Pace S, Polichetti M. 2019. Pinning energy and anisotropy properties of a Fe(Se,Te) iron based superconductor. Nanotechnology 30: 254001.

Galluzzi A, Mancusi D, Cirillo C, Attanasio C, Pace S, Polichetti M. 2018b. Determination of the Transition Temperature of a Weak Ferromagnetic Thin Film by Means of an Evolution of the Method Based on the Arrott Plots. J. Supercond. Nov. Magn. 31: 1127–1132.

Hergt R, Dutz S, Müller R, Zeisberger M. 2006. Magnetic particle hyperthermia: nanoparticle magnetism and materials development for cancer therapy. J. Phys. Condens. Matter 18: S2919–S2934.

Ho BT, Roberts TK, Lucas S. 2018. An overview on biodegradation of polystyrene and modified polystyrene: the microbial approach. Crit. Rev. Biotechnol. 38: 308–320.

Horst MF, Alvarez M, Lassalle VL. 2016. Removal of heavy metals from wastewater using magnetic nanocomposites: Analysis of the experimental conditions. Sep. Sci. Technol. 51: 550–563.

Huang J, Bu L, Xie J, Chen K, Cheng Z, Li X, Chen X. 2010. Effects of nanoparticle size on cellular uptake and liver MRI with polyvinylpyrrolidone-coated iron oxide nanoparticles. ACS Nano 4: 7151–7160.

Iannone G, Zola D, Armenio AA, Polichetti M, Attanasio C. 2007. Electrical resistivity and magnetic behavior of PdNi and CuNi thin films. Phys. Rev. B - Condens. Matter Mater. Phys. 75: 064409.

Kalia S, Kango S, Kumar A, Haldorai Y, Kumari B, Kumar R. 2014. Magnetic polymer nanocomposites for environmental and biomedical applications. Colloid Polym. Sci. 292: 2025–2052.

Kim D-H, Rozhkova EA, Ulasov I V., Bader SD, Rajh T, Lesniak MS, Novosad V. 2010. Biofunctionalized magnetic-vortex microdiscs for targeted cancer-cell destruction. Nat. Mater. 9: 165–171.

Kumar CSSR, Mohammad F. 2011. Magnetic nanomaterials for hyperthermia-based therapy and controlled drug delivery. Adv. Drug Deliv. Rev. 63: 789–808.

Lerman MJ, Lembong J, Muramoto S, Gillen G, Fisher JP. 2018. The Evolution of Polystyrene as a Cell Culture Material. Tissue Eng. Part B Rev. 24: 359–372.

Murariu M, Dubois P. 2016. PLA composites:From production to properties. Adv. Drug Deliv. Rev. 107: 17–46.

Oh JK, Park JM. 2011. Iron oxide-based superparamagnetic polymeric nanomaterials: Design, preparation, and biomedical application. Prog. Polym. Sci. 36: 168–189.

Di Palma L, Bavasso I, Sarasini F, Tirillò J, Puglia D, Dominici F, Torre L, Galluzzi A, Polichetti M, Ramazanov MA, Hajiyeva F V., Shirinova HA. 2018. Effect of nano-magnetite particle content on mechanical, thermal and magnetic properties of polypropylene composites. Polym. Compos. 39: E1742–E1750.

Pankhurst QA, Connolly J, Jones SK, Dobson J. 2003. Applications of magnetic nanoparticles in biomedicine. J. Phys. D. Appl. Phys. 36: R167–R181.

Polichetti M, Modestino M, Galluzzi A, Pace S, Iuliano M, Ciambelli P, Sarno M. 2020. Influence of citric acid and oleic acid coating on the dc magnetic properties of Fe3O4 magnetic nanoparticles. Mater. Today Proc. 20: 21–24.

Dos Santos LM, Ligabue R, Dumas A, Le Roux C, Micoud P, Meunier JF, Martin F, Einloft S. 2015. New magnetic nanocomposites: Polyurethane/ Fe3O4-synthetic talc. Eur. Polym. J. 69: 38–49.

Shannigrahi SR, Pramoda KP, Nugroho FAA. 2012. Synthesis and characterizations of microwave sintered ferrite powders and their composite films for practical applications. J. Magn. Magn. Mater. 324: 140–145.

Shirinova H, Di Palma L, Sarasini F, Tirillò J, Ramazanov MA, Hajiyeva F, Sannino D, Polichetti M, Galluzzi A. 2016. Synthesis and characterization of magnetic nanocomposites for environmental remediation. Chem. Eng. Trans. 47: 103–108.

Veiseh O, Gunn JW, Zhang M. 2010. Design and fabrication of magnetic nanoparticles for targeted drug delivery and imaging. Adv. Drug Deliv. Rev. 62: 284–304.

Wilson JL, Poddar P, Frey NA, Srikanth H, Mohomed K, Harmon JP, Kotha S, Wachsmuth J. 2004. Synthesis and magnetic properties of polymer nanocomposites with embedded iron nanoparticles. J. Appl. Phys. 95: 1439–1443.

Yan X, He Q, Zhang X, Gu H, Chen H, Wang Q, Sun L, Wei S, Guo Z. 2014. Magnetic Polystyrene Nanocomposites Reinforced with Magnetite Nanoparticles. Macromol. Mater. Eng. 299: 485–494.

Zhang H wang, Liu Y, Sun S heng. 2010. Synthesis and assembly of magnetic nanoparticles for information and energy storage applications. Front. Phys. China 5: 347–356.

Zhu J, Wei S, Chen M, Gu H, Rapole SB, Pallavkar S, Ho TC, Hopper J, Guo Z. 2013. Magnetic nanocomposites for environmental remediation. In: Advanced Powder Technology. Elsevier, p 459–467.